Available online at www.sciencedirect.com
SCIENCE DIRECT®
Biochemical Pharmacology 68 (2004) 2367–2378
Biochemical Pharmacology
www.elsevier.com/locate/biochempharm

Effects and regulation of osteopontin in rat hepatic stellate cells

Sung Hee Lee[a], Geom Seog Seo[b], Young Nyun Park[c], Tae Moo Yoo[d], Dong Hwan Sohn[a,*]

[a]*Medicinal Resources Research Center, College of Pharmacy, Wonkwang University, Iksan, Jeonbuk 570-749, Republic of Korea*
[b]*Department of Internal Medicine, Wonkwang University Medical School, Iksan, Jeonbuk 570-749, Republic of Korea*
[c]*Department of Pathology and Brain Korea 21 project for Medical Science, Center for Chronic Metabolic Disease Research, Yonsei University College of Medicine, Seoul 120-749, Republic of Korea*
[d]*National Institute of Toxicological Research, Korea Food and Drug Administration, Seoul 122-704, Republic of Korea*

Received 23 June 2004; accepted 17 August 2004

Abstract

Using a cDNA microarray, we identified osteopontin (OPN) as one of the genes upregulated in cultured activated hepatic stellate cells (HSCs). Northern and western blot analyses showed that OPN was increasingly expressed during the progressive activation of cultured rat HSCs, and a significant increase in OPN was observed in carbon tetrachloride-induced rat liver fibrosis. In biliary atresia, OPN protein was predominantly expressed in Kupffer cells and HSCs in the necrotic areas. Incubation of HSCs with recombinant OPN-induced significant proliferative and migratory effects, and induced matrix metalloproteinase 2 production and activation. Moreover, OPN increased type I collagen production and type II transforming growth factor-β receptor mRNA and protein. In conclusion, this study shows that OPN is expressed in activated HSCs and suggests that the upregulation of OPN might be a central pathway of HSC activation.
© 2004 Elsevier Inc. All rights reserved.

Keywords: Hepatic stellate cell; cDNA microarray; Osteopontin; MMP-2; Type I collagen; Type II TGF-β; receptor

1. Introduction

Hepatic fibrosis, or scar deposition in response to chronic injury, is similar in all forms of liver disease [1]. Accumulation of fibrillar, or type I collagen occurs in the subendothelial space between hepatocytes and endothelial cells, where it replaces a low-density basement membrane-like matrix containing type IV collagen. This conversion of the subendothelial matrix to one rich in fibrillar collagen is a pivotal event mediating the loss of differentiated function that is characteristic of progressive liver disease [2,3].

The perisinusoidal hepatic stellate cell (HSC) is largely responsible for the increase in extracellular matrix (ECM) deposition. The HSC is transformed after a fibrogenic stimulus from a quiescent cell type to an activated cell type. The accumulation of type I collagen has a direct activating effect on HSCs [4]. Stellate cell activation is further accelerated by upregulation of matrix metalloproteinase 2 (MMP-2) activity, because this enzyme degrades the normal subendothelial matrix, hastening its replacement by fibrillar collagen [5]. The activity of MMP-2 is tightly regulated by specific inhibitors, including tissue inhibitor of metalloproteinase 2 (TIMP-2), and by activators including membrane type 1 matrix metalloproteinase (MT1-MMP) [6,7].

Osteopontin (OPN) is a secreted glycoprotein with a multidomain structure and functions characteristic of matricellular protein [8,9]. It has an *N*-terminal signal sequence, a highly acidic region consisting of nine consecutive aspartic acid residues, and a GRGDS cell-adhesion sequence predicted to be flanked by the β-sheet structures [10]. This protein has a functional thrombin cleavage site and is a substrate for tissue transglutaminase [9]. OPN binds to type I collagen [11], fibronectin [12], and osteocalcin [13]. It causes cell adhesion, cell migration, ECM-invasion, and cell proliferation by interacting with its

Abbreviations: ECM, extracellular matrix; MMP-2, matrix metalloproteinase 2; MTI-MMP, membrane type I matrix metalloproteinase; OPN, osteopontin; PDGF, platelet-derived growth factor; TGF-β, transforming growth factor β; TβRII, type II TGF-β; receptor; TIMP-2 t, issue inhibitor of metalloproteinase 2

* Corresponding author. Tel.: +82 63 850 6822; fax: +82 63 854 6038.
E-mail address: dhsohn@wonkwang.ac.kr (D.H. Sohn).

0006-2952/$ – see front matter © 2004 Elsevier Inc. All rights reserved.
doi:10.1016/j.bcp.2004.08.022

receptor, αvβ3 integrin, in various cell types [14]. The role of OPN in liver diseases is undefined. Carbon tetrachloride administration in the rat has been shown to increase OPN expression in liver where it was localized mainly to Kupffer cells, macrophages, and HSCs [15]. Recombinant OPN also stimulated hepatic macrophage migration in vitro. These data suggest that OPN could play an important role in recruiting inflammation to the liver. Recent studies have also shown markedly increased OPN gene expression in human hepatocellular carcinoma, which suggests that hepatocytes can synthesize OPN [16,17]. These limited findings led us to consider the hypothesis that OPN may play a role in the activation of HSCs. Of interest, in this study, we identified OPN as one member of the genes that are upregulated in cultured activated HSCs, using a rat cDNA microarray. Therefore, the purpose of this study was to identify OPN and to determine the role of OPN in HSCs.

2. Materials and methods

2.1. HSC isolation and culture

Rat HSCs were isolated from the livers of Sprague–Dawley rats as described previously [18,19]. In the present study, freshly isolated HSCs from normal liver were referred to as quiescent HSCs. Likewise, HSCs isolated from normal liver and cultured for 14 days were referred to as in vitro activated HSCs.

After reaching confluency (about 14 days after plating), activated HSCs were detached by incubation with trypsin (0.025% trypsin/0.5 mM EDTA), and subcultured. Experimental manipulations were performed on cells between the third and fifth serial passages.

2.2. Genechip analysis

Total RNA was purified from cells using TRIzol reagent™ (Invitrogen) following the manufacturer's instructions. All procedures were performed according to the instructions of GenomicTree, Inc. (Daejon, South Korea). RNA from the quiescent HSCs was labeled with cyanine 3-dUTP (Cy3-dUTP, NEN Life Science Products) and then used as the control target. RNA from activated HSCs was labeled separately with cyanine 5-dUTP (Cy5-dUTP, NEN Life Science Products) and was used as a tester. The cDNA targets were synthesized from total RNAs in the presence of either Cy3-dUTP (for quiescent HSCs) or Cy5-dUTP (for activated HSCs) and applied to the cDNA microarray. The labeled cDNAs were then purified through a Microcon-30 column and resuspended in 80 μl of hybridization solution (3× SSC and 0.3% SDS). The target mixture was denatured at 100 °C for 2 min and applied to the chip (RSVC321; GenomicTree, Inc.) at 65 °C for 16 h in a humidified chamber. The hybridized slide was washed in 2× SSC for 2 min, 0.1× SSC/0.1% SDS for 5 min, and 0.1× SSC for 5 min, and then spin-dried at room temperature before scanning.

Microarray scanning and normalization of the data were performed using a GenePix 4000B scanner and GenePix pro 3.0 software package (http://www.axon.com/). Poor quality spots (sum of median intensity <500) were filtered from the raw data before analysis. For each hybridized spot, a gene expression value (GEV; ratio of median fluorescence intensity in GenePix pro 3.0), the ratio of Cy5 fluorescence intensity minus Cy5 background intensity to Cy3 fluorescence intensity minus Cy3 background intensity, was calculated and represents the fold change in expression for each gene. The cDNA microarray experiments were repeated twice under each set of conditions and the average of two GEVs for each gene was used in the analysis.

2.3. Experimental fibrotic model

Liver fibrosis was induced in pathogen-free male Sprague–Dawley rats (200–250 g). Rat livers were obtained from rats treated with carbon tetrachloride (CCl_4), using the dosing regimen described previously [18–20]. The CCl_4 group ($n = 6$) was treated with an oral administration of CCl_4 (Sigma Chemical) diluted 50% (v/v) with corn oil (Sigma Chemical) at a dose of 1 ml/kg body weight for each rat. CCl_4 was administrated twice per week for six weeks. Three days after the last CCl_4 treatment, the rats were sacrificed; control animals ($n = 6$) were treated with corn oil for six weeks. All animals received humane care according to National Institute of Health guidelines.

2.4. Northern blot analysis

Total RNA (20 μg) was separated electrophoretically on a 1% agarose gel containing 5.4% formaldehyde, transferred to nylon membranes (Hybond-N; Amersham Pharmacia Biotech) by electroblotting, and fixed with UV irradiation. The RNA was hybridized with randomly primed [^{32}P]-cDNA-specific for OPN, transforming growth factor-β (TGF-β), or GAPDH. OPN and TGF-β cDNAs amplified by RT-PCR corresponded to bases 80–923 of the rat OPN sequence (GenBank accession no. M14656) and bases 820–1046 of the rat TGF-β sequence (GenBank accession no. X52498), respectively. Purified PCR products were sequenced to confirm gene identity. Prehybridization and hybridization were performed at 68 °C, and the membranes were then washed as described previously [18]. Reactive bands were detected by autoradiography using X-ray film (Agfa).

2.5. Reverse transcriptase- polymerase chain reaction (RT-PCR)

Total RNA (5 μg) was reverse-transcribed using the Moloney Murine Leukemia Virus reverse transcriptase (Gibco BRL) and the resultant cDNA was diluted 10-fold

for PCR. Oligonucleotide primer sequences were as follows: rat MMP-2 sense, 5′-gtt ggc agt gca ata cct ga-3′ (corresponding to nt 435–454) and antisense, 5′-agg cat cat cca ctg tct ca-3′ (corresponding to 702–721), according to GenBank accession no. U65656; and rat type II TGF-β receptor sense, 5′-cac tgt cca ctt gtg aca ac-3′ (corresponding to nt 228–247) and antisense, 5′-ggt ctc aaa ctg ctc tga ag-3′ (corresponding to nt 858–877), according to GenBank accession no. L09653. PCR reactions were carried out in the presence of 1.5 mM $MgCl_2$ for 30 cycles at the following temperatures and times: denaturation at 94 °C for 30 s; annealing at 55 °C for 30 s for MMP-2, and 56 °C for 30 s for type II TGF-β receptor; extension at 72 °C for 1 min; these cycles were followed by a final extension at 72 °C for 10 min.

The amplified PCR products were analyzed by agarose gel electrophoresis with ethidium bromide staining. The integrity of cDNA samples was confirmed using primers specific for rat GAPDH [18]. Purified PCR products were sequenced using an autosequencer (ABI 377 DNA sequencer; Perkin-Elmer) and these sequences were compared with those in the BLAST nucleotide program (blastn) to confirm gene identity.

2.6. Immunohistochemistry

For human liver tissues with biliary cirrhosis, immunohistochemical studies were performed using a catalyzed signal amplification system (Dako), as described previously [18]. There were two cases of biliary atresia from the explanted livers of a two-year-old girl and a three-year-old boy, and a case of primary biliary cirrhosis from the explanted liver of a 42-year-old woman. For the control, normal liver tissue, obtained from a liver resected for hemangioma in a 44-year-old woman, was used. The control had no hepatitis virus and showed normal liver histology. These sample sections were incubated at 4 °C overnight with primary monoclonal antibody against human OPN (500 ng/ml, clone MPIIIB101, hybridoma supernatant; Development Studies Hybridoma Bank). 3-Amino-9-ethylcarbazole was used as the colorizing agent and counterstaining was performed with Harris' hematoxylin.

2.7. Cell proliferation analysis

Cell proliferation was evaluated by bromodeoxyuridine (BrdU) incorporation using an ELISA kit (Roche Applied Science) [21]. HSCs were plated onto a 96-well microtiter plate at a density of 2×10^4 cells/well, washed three times in serum-free WME, and left in this medium for 1 h after the final wash. The cells were then incubated in fresh medium containing 0.01% FBS for 24 h. Serum-starved HSC cells were incubated in the absence or presence of increasing concentrations of recombinant mouse OPN (R&D Systems) at 37 °C for another 24 h, including a 6-h pulse labeling with BrdU. After the culture medium had been removed, the cells were fixed, incubated with anti-BrdU antibody conjugated with peroxidase, and the incorporated BrdU was detected with a subsequent substrate reaction according to the manufacturer's instructions.

2.8. Migration analysis

For the chemotaxis assay, we used modified Transwell cell-culture chamber with an 8-μm pore filter (Corning Costar Corporation) coated with type I collagen (Sigma Chemical) to facilitate cell movement [22,23]. Briefly, the filter was coated with type I collagen by immersing it for 1 min in collagen type I solution (100 μg/ml in 0.5 M acetic acid), then drying it for 15 min at room temperature under sterile conditions. Confluent HSCs were serum-starved for 24 h, trypsinized, and resuspended in serum-free medium containing 1% albumin, and then added to the upper chamber. The lower chamber was filled with serum-free medium supplemented with 1% bovine serum albumin (control) or platelet-derived growth factor (PDGF)-BB (10 ng/ml) or three different concentrations of recombinant mouse OPN. After incubation at 37 °C for 24 h, the nonmigrated cells on the upper surface of the filters were scraped and washed off. After fixing with 2.5% glutaraldehyde and staining with Gill's hematoxylin solution, the cells that had migrated to the underside of the filters were quantified as the mean number of cells in 10 high-power fields.

2.9. Wound healing assay

To measure cell migration during wound healing [24,25], HSCs were seeded onto 24-well plates coated with gelatin (Sigma Chemical) and grown to confluence in WME medium containing 10% FBS. Confluent cell cultures were incubated in serum-free medium for 24 h before commencement of the experiment. Monolayers were then disrupted with a cell scraper to generate a linear wound of ≅1 mm, then washed to remove debris, and incubated in medium containing 10% FBS with or without anti-mouse OPN antibody (R&D Systems). Cells were photographed after wounding under phase contrast microscopy. To evaluate 'wound closure' under the different experimental conditions, five randomly selected points along each wound were marked and the horizontal distance between the migrating cells and the initial wound was measured at 24 h after wounding.

2.10. Western blot analysis

Equal volumes of conditioned medium from HSCs were concentrated 10-fold in 10 kDa microcentrifuge concentrators (Millipore). Equal amounts of protein were resolved on SDS-polyacrylamide gel electrophoresis, blotted onto a nitrocellulose membrane (Amersham Pharmacia Biotech), and incubated with a primary antibody: anti-mouse OPN antibody (R&D Systems) diluted 1:500, anti-MMP-2 anti-

body (Chemicon International) diluted 1:2000, anti-TIMP-2 antibody (Chemicon International) diluted 1:200, or anti-type I collagen antibody (Calbiochem) diluted 1:200.

Cells were washed twice with Hanks's balanced salt solution and lysed directly in RIPA buffer (50 mM Tris–HCl (pH 7.4), 1% (v/v) Triton X-100, 1 mM EDTA, 1 mM leupeptin, 1 mM phenylmethylsulfonyl fluoride). The lysates were centrifuged at 14,000 rpm for 30 min at 4 °C and the supernatants collected. Cell lysate (20 μg) was separated by SDS-polyacrylamide gel electrophoresis, blotted onto nitrocellulose membrane, and incubated with a primary antibody: anti-MT1-MMP (Chemicon International) diluted 1:1000 or anti-type II TGF-β receptor (Santa Cruz Biotechnology) diluted 1:200.

After repeated washing, the membranes were incubated with horseradish-peroxidase-conjugated anti-goat, anti-rabbit, or anti-mouse secondary antibody (Santa Cruz Biotechnology) diluted 1:2000. The bands were visualized using the enhanced chemiluminescence (ECL) system (Amersham Pharmacia Biotech).

2.11. Gelatin zymography

Zymographic analyses were performed on the conditioned media from cultured HSCs [26]. Conditioned media normalized to equal cell numbers were concentrated 10-fold in 10 kDa microcentrifuge concentrators (Millipore). An aliquot of each sample was mixed with an equal volume of 2× SDS sample buffer in the absence of reducing agent, and incubated for 30 min at room temperature. The samples were separated electrophoretically on 10% polyacrylamide gels copolymerized with 0.2% gelatin. After electrophoresis, the gel was washed twice with 2.5% Triton X-100 for 30 min at room temperature. After being washed, the gel was incubated for 16 h at 37 °C in developing buffer (50 mM Tris–HCl (pH 8.0), 50 mM $CaCl_2$, 1 μM $ZnCl_2$). The gel was then stained with 1% Coomassie brilliant blue G250 and destained with 10% methanol and 7.5% acetic acid. The zones of gelatinolytic activity were visualized by negative staining. Results were quantified by scanning densitometry analysis.

2.12. Statistics

Data were analyzed with one-way ANOVA and Tukey's multiple comparison tests when comparing means of more than three. Calculations were performed with the GraphPad Prism program (GraphPad Software).

3. Results

3.1. Expression of OPN in cultured rat HSCs

In this study, we used cDNA microarray experiments to categorize the genes with altered expression levels during the activation of rat HSCs. Of the 5088 genes screened, 54 genes were upregulated more than 10-folds in activated HSCs (Table 1). Several lines of evidence have been accumulated regarding the HSC activation. Not surprisingly, most of the highly upregulated gene was αB-crystallin. αB-crystallin have been reported to upregulate following activation in human and rat HSCs [27,28]. Additionally, this study recapitulated previous observation using proteome analysis [29]. β-Galactoside-binding lectin has been reported that the mRNA level was increased in both in vivo and in vitro activated HSCs.

One of the strongly upregulated genes was that encoding OPN, with a 17.8-fold increase in expression. We performed northern blot analysis to confirm OPN mRNA expression during the progressive activation of rat HSCs in culture. As shown in Fig. 1A, OPN mRNA was virtually undetectable in cellular RNA prepared from quiescent HSCs, but increased significantly following HSC activation. Moreover, these results indicate that a qualitative correlation exists between northern analysis and the microarray data.

To complement the above studies of mRNA expression, immunoblotting was used to detect OPN in cultured HSCs. Western blot analysis was performed on concentrated conditioned medium from primary cultures of activated HSCs (cultured for seven days). The concentrated medium showed specific binding of anti-OPN antibody to a ≅65 kDa major band (Fig. 1B). This band was not detectable in the conditioned medium from quiescent HSCs, but the intensity of the band increased with progressive HSCs activation in culture.

3.2. Expression of OPN in CCl_4-treated rat liver and human liver

To determine whether OPN is induced during liver injury in vivo and to determine the expression levels of OPN during progressive liver fibrosis, we analyzed OPN mRNA, induced in rat liver by CCl_4 treatment. This model of liver injury has been used extensively to characterize stellate cell activation in vivo. Fig. 2 shows negligible expression of OPN mRNA in the control livers, whereas significant expression is seen in the CCl_4-induced fibrotic livers. In the CCl_4-treated livers, OPN mRNA was readily detectable after two weeks of CCl_4 treatment, with expression reaching a maximum after six weeks of treatment, similar to the expression pattern for TGF-β mRNA. This finding confirms that the expression of OPN mRNA increases with the increasing severity of liver fibrosis.

OPN was also detected by immunohistochemistry in fibrotic human liver (Fig. 3). In primary biliary cirrhosis, OPN immunoreactivity was strong in the inflammatory cells, as described previously [30], in contrast to negative reaction in normal liver. Moreover, in biliary cirrhosis due to biliary atresia, marked OPN signal was found in Kupffer cell (arrow head) and HSCs (arrow) in the necrotic areas. No staining was observed when primary antibody was omitted.

Table 1
Genes upregulated more than 10-fold in expression between quiescent and activated stellate cells

Gene name	GenBank#	GEV[a]
Genes upregulated more than 40-fold		
Alpha-crystallin B chain	AA818795	74.9
EST	AA900319	72.9
ESTs	AA900234	70.7
SM22	AA819452	54.4
Platelet factor 4 (PF4)	AA956032	52.9
Desmin	AA819161	52.6
Lung β-galactoside binding lectin	AA859699	52.0
Lysyl oxidase	AA925828	48.0
Calpain small subunit	AA900053	44.9
EST	AA901383	44.7
Calponin	AI045937	41.4
Genes upregulated more than 30-fold		
Pancreatic secretory trypsin inhibitor type II	AA858673	39.6
ESTs	AA818700	39.2
ESTs	AA818967	38.1
ESTs	AA924334	36.1
Genes upregulated more than 20-fold		
Rho-associated kinase	AI137331	26.6
Cytochrome P4501b1	AI060107	25.8
Protein F1	AI043649	25.7
ESTs, weakly similar to isocitrate dehydrogenase beta subunit	AA900150	24.9
ESTs, highly similar to hypothetical 43	AA899751	23.7
ESTs	AA901043	23.7
MIFR	AA900609	22.3
ESTs	AA817883	21.5
ESTs	AI111919	21.0
Ribosomal protein L21	AA819765	20.9
ESTs, weakly similar to 5-lipoxygenase A	AI111907	20.4
Genes upregulated more than 10-fold		
ESTs, weakly similar to tropomyosin	AA858875	19.6
Follistatin	AA858520	19.1
ESTs	AA997748	18.9
Neuronal protein (NP25)	AI044424	18.7
γ-subunit of sodium potassium ATPase	AA924590	18.7
unc-50-related protein	AA923854	18.6
Annexin 1	AA964960	18.4
Collagen alpha 1 type I	AA924727	17.9
Osteopontin	AA964431	17.8
Neuron specific enolase	AA997308	17.7
γ-Enteric smooth muscle actin isoform	AA817767	17.5
ESTs	AA858733	16.0
ESTs, moderately similar to laminin B2 chain	AA900866	14.8
Carbonic anhydrase II	AA926296	14.3
ESTs	AA899090	13.7
ESTs	AA955299	13.5
ESTs	AA924552	13.2
Drs (a gene downregulated by v-src)	AA818824	12.9
Subtilisin-like endoprotease	AA956778	12.8
Creatine kinase	AA818791	12.4
DAP-like kinase	AA859438	12.1
ESTs	AA818863	12.0
Integral membrane glycoprotein	AI029064	11.9
ESTs	AA818572	11.9
Nuclear serine/threonin kinase	AA866455	11.7
EST	AA901243	11.6
ESTs, highly similar to Lsm3 protein	AA901259	10.9
Vimentin	AA859385	10.2

[a] For GEV, 10 means a 10-fold upregulation. Information about gene function can be obtained by using GenBank# in the table at http://genome-www5.stanford.edu/cgi-bin/SMD/source/sourceSearch/.

3.3. OPN promotes stellate cell proliferation and migration

Although fibrogenesis is mainly the result of HSC activation, proliferation and migration are important functions gained by HSC during activation and are of major importance in the development of fibrosis [31]. To assess the effects of OPN on HSCs, we used established in vitro assay systems to evaluate the effects of this protein on proliferation and migration.

To examine whether OPN has any role in the growth rate of these cells, we performed a proliferation assay by comparing the incorporation of BrdU in HSCs incubated with different doses of recombinant OPN. The results indicate that OPN induces BrdU incorporation of HSCs in a dose-dependent manner. A significant increase was observed with OPN concentrations of 3 and 6 μg/ml compared with the control treatment (Fig. 4A).

To assess the effects of OPN on migration, HSCs were seeded in the upper compartment of a Transwell chamber and were allowed to migrate through the filter in response to recombinant OPN. In the presence of OPN, HSC migration increased under all conditions tested. Fig. 4B shows the dose-dependent increases in cell migration with increasing concentrations of OPN in the lower chamber. These data suggest that OPN induces the migration of HSCs by chemotaxis.

3.4. Antibody directed against OPN inhibits wound healing migration

The wound healing migration assay is an established and widely used procedure that allows cell migration to be monitored at different intervals of time in response to an artificial wound produced on a cell monolayer. Furthermore, this method allows the observation of changes in cell morphology that may occur during this process [32]. No change was observed when the cells were incubated in serum-free medium (data not shown). As shown in Fig. 4C, incubation of cells with 10% FBS produced marked cell migration into the wound area, reaching a level of 'wound closure' at 24 h after wounding (Fig. 4C, panel b), whereas cell migration was markedly reduced when anti-OPN antibody were applied (Fig. 4C, panels c and d). The percentage inhibition of wound closure, evaluated over the whole wound length, was 26% for 2 μg/ml anti-OPN antibody and 40% for 5 μg/ml anti-OPN antibody.

3.5. OPN promotes MMP-2 expression and activity in stellate cells

We examined whether OPN stimulates MMP-2 expression in HSCs. Conditioned media were collected, and MMP-2 expression was detected by immunoblotting. Increased levels of MMP-2 expression were observed when the cells were treated with two different concentrations of OPN (Fig. 5A, panel a). Compared with controls,

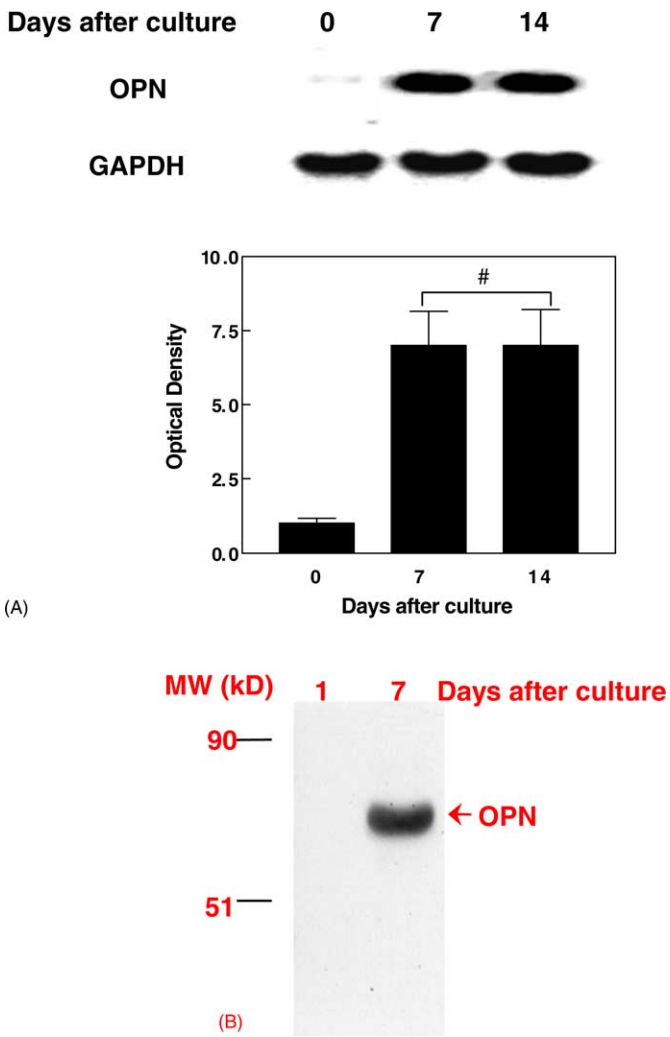

Fig. 1. Expression of OPN in HSCs. (A) OPN mRNA expression was determined by northern blotting using GAPDH mRNA to control for sample loading. Total cellular RNA was prepared from freshly isolated HSCs, or from HSCs that had been cultured in 10% FBS-containing medium on plastic for the times shown. A representative northern blot is shown. Results are means ± S.D. from three independent experiments. The OPN mRNA densitometry values were normalized to their respective GAPDH densitometry values. Statistical significance: $^{\#}p < 0.05$ vs. 0 day, as analyzed by one-way ANOVA and Tukey's multiple comparison tests. (B) Identification of OPN in culture media by western analysis using anti-OPN antibody. Concentrated conditioned media from HSCs that had been cultured for one day or seven days were examined. Note the virtual absence of OPN in the conditioned medium from one-day-cultured HSCs and the highly conspicuous OPN bands in the conditioned medium from seven-day-cultured HSCs.

there were at least three- and four-fold increases in MMP-2 expression when the cells were treated with 1 and 3 μg/ml OPN, respectively.

A zymography assay revealed a band of gelatin degradation at 72 kDa, representing latent MMP-2, and a faint band at 68 kDa, representing active MMP-2 (Fig. 5A, panel b). These results show that the levels of MMP-2 gelatinase activity were higher in OPN-treated cells than in untreated cells. Gelatinase activity was confined to the medium and none was observed in cell lysates (data not shown).

OPN-induced MMP-2 expression in these cells was confirmed by RT-PCR. The intensity of the MMP-2 specific band increased when the cells were treated with OPN (Fig. 5B). The level of MMP-2 mRNA was also quantified by densitometry and analyzed statistically. There was an increase of at least 2.8-fold in MMP-2 expression when the cells were treated with 3 μg/ml OPN compared with control cells. These data were corroborated by immunoblotting and zymography data.

3.6. OPN induces TIMP-2 and MT1-MMP expression in stellate cells

Because TIMP-2 and MT1-MMP, together with MMP-2, comprise a trimolecular complex that collectively regulates MMP-2 activity [7], we examined whether OPN has any role in the induction of TIMP-2 or MT1-MMP expression in HSCs.

Conditioned media were collected, and TIMP-2 expression was detected on western blot using anti-TIMP-2 antibody. The data indicate that the level of TIMP-2 expression (24 kDa) increased 12- and 18-fold when the cells were treated with 1 and 3 μg/ml OPN, respectively, compared with control cells (Fig. 6A).

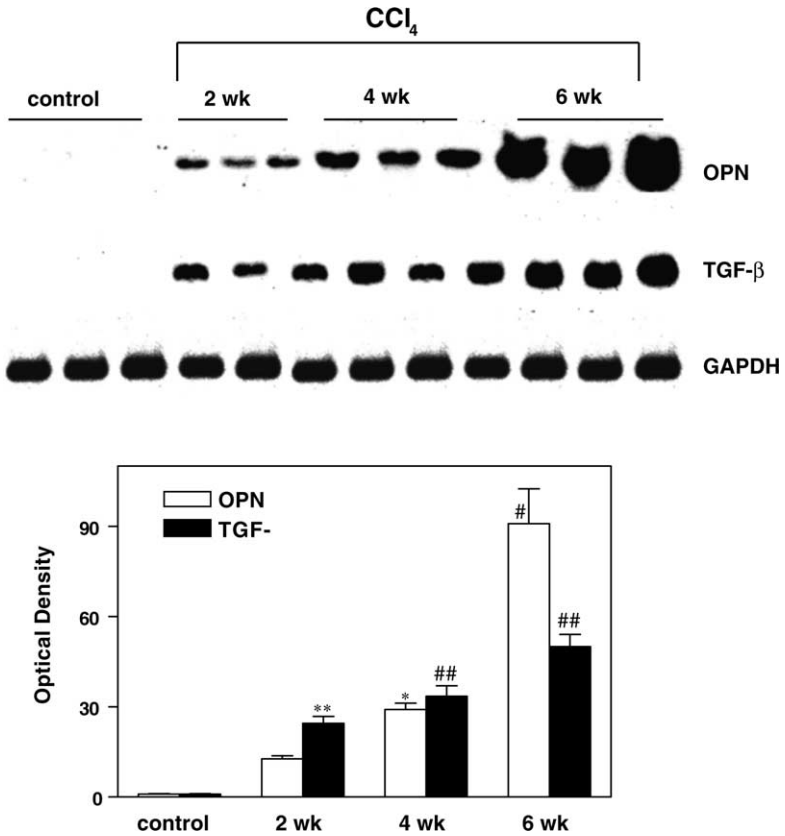

Fig. 2. Northern blot analysis of OPN and TGF-β mRNAs from the livers of rats treated with corn oil (control) or CCl_4 for the indicated weeks. Liver tissue collected from three individual animals was tested. Results are means ± S.D. from three individual animals. The OPN and TGF-β mRNA densitometry values were normalized to their respective GAPDH densitometry values. Statistical significance: $^{*}p < 0.05$ and $^{\#}p < 0.001$ vs. the control for OPN; $^{**}p < 0.01$ and $^{\#\#}p < 0.001$ vs. the control for TGF-β, as analyzed by one-way ANOVA and Tukey's multiple comparison tests.

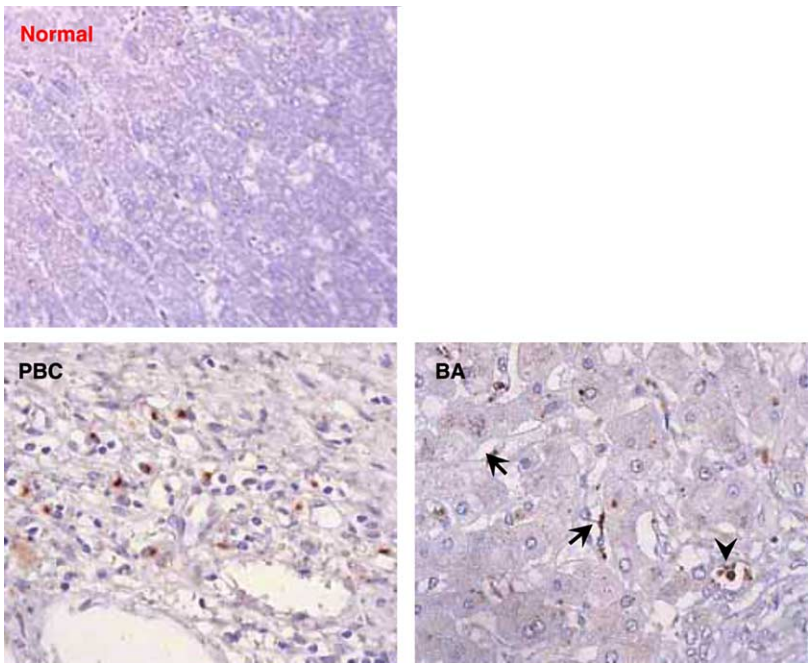

Fig. 3. Detection of OPN expression by immunohistochemistry. In normal liver, OPN-positive cells were very few. Primary biliary cirrhosis (PBC) showed a positive reaction in the inflammatory cells. Biliary atresia (BA) showed a positive reaction in Kupffer cell (arrow head) and HSCs (arrows) in the necrotic areas. Original magnification: 400×.

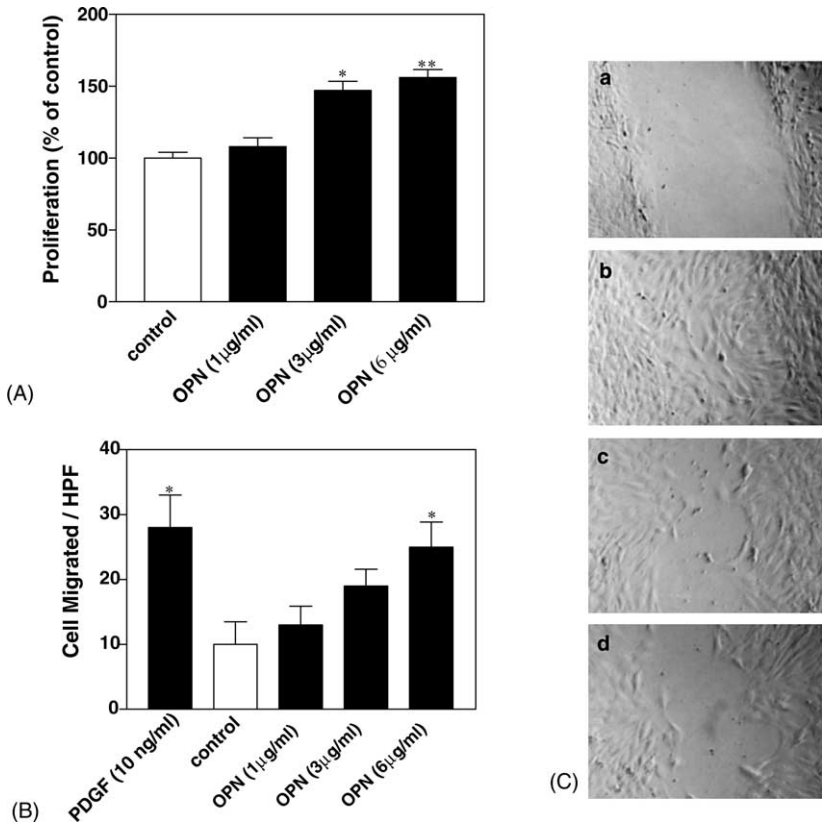

Fig. 4. (A) Effect of OPN on the proliferation of stellate cells. HSCs were incubated in the presence of recombinant OPN (0, 1, 3, or 6 μg/ml) for 24 h. Cells were incubated with 5-bromo-2′-deoxyuridine (BrdU) for 6 h. Results are the means ± S.D. of three independent experiments, each performed using triplicate wells. Statistical significance: $^{*}p < 0.01$ and $^{**}p < 0.001$ vs. control conditions, as analyzed by one-way ANOVA and Tukey's multiple comparison tests. (B) HSC migration through porous membrane after addition of OPN. Recombinant OPN was added to the lower compartment of a Transwell cell-culture chamber. The values (cells migrated per high-power field) are expressed as means ± S.D. of three independent experiments, each performed using triplicate wells. Statistical significance: $^{*}p < 0.05$ vs. control conditions, as analyzed by one-way ANOVA and Tukey's multiple comparison tests. (C) Inhibitory effects of anti-OPN antibody on HSC motility in a wound healing model. A scrape wound was generated in the cell layer to remove a linear area of cells (a), the culture was allowed to migrate for 24 h and close the wound in the presence of 10% FBS (b), FBS + 2 μg/ml anti-OPN antibody (c), or FBS + 5 μg/ml anti-OPN antibody (d). Cells were photographed after wounding under phase contrast microscopy and measurements were performed as indicated in Section 2. Representative result from two independent experiments.

The cells were lysed, and the level of MT1-MMP was determined by immunoblotting. The densitometric data indicate that there was an increase in MT1-MMP expression in the OPN-treated cells compared with control cells (Fig. 6B).

3.7. Effect of OPN on α1(I) collagen expression

Type I collagen has an activating effect on HSCs [4] and HSC activation is further accelerated by the upregulation of MMP-2 activity [5]. Therefore, we examined whether OPN has any direct effect on type I collagen expression. The effect of OPN on type I collagen production was determined in concentrated conditioned medium by immunoblotting. The results indicate that OPN induces type I collagen expression in a dose-dependent manner in HSCs. A significant increase was observed when cells were treated with OPN compared with cells cultured under control conditions (Fig. 7A).

Stellate cells produce TGF-β1, which is known to stimulate collagen formation [33,34]. TGF-β signaling is initiated by the binding of this active cytokine to the type II TGF-β receptor (TβRII) [35]. Here, we investigated whether OPN causes any change in TGF-β1 or its type II receptor. OPN exposure did not change significantly TGF-β1 mRNA determined by RT-PCR in the HSCs (data not shown). By contrast, exposure of the HSCs to 1 and 3 μg/ml OPN resulted in a 1.5- and 2.5-fold increase in TβRII mRNA, respectively, determined by RT-PCR (Fig. 7B, panel a). Exogenous OPN induced an increase in TβRII protein, determined by immunoblotting. The increases in TβRII in cells treated with OPN concentrations of 1 and 3 μg/ml were 2.3- and 3.3-fold, respectively (Fig. 7B, panel b).

4. Discussion

The activation of HSCs is a key step in the development of liver fibrosis [36–39]. Several factors are upregulated in activated stellate cells, which are thought to contribute to the development of fibrosis [40]. Analysis of the differences in gene expression between quiescent and activated

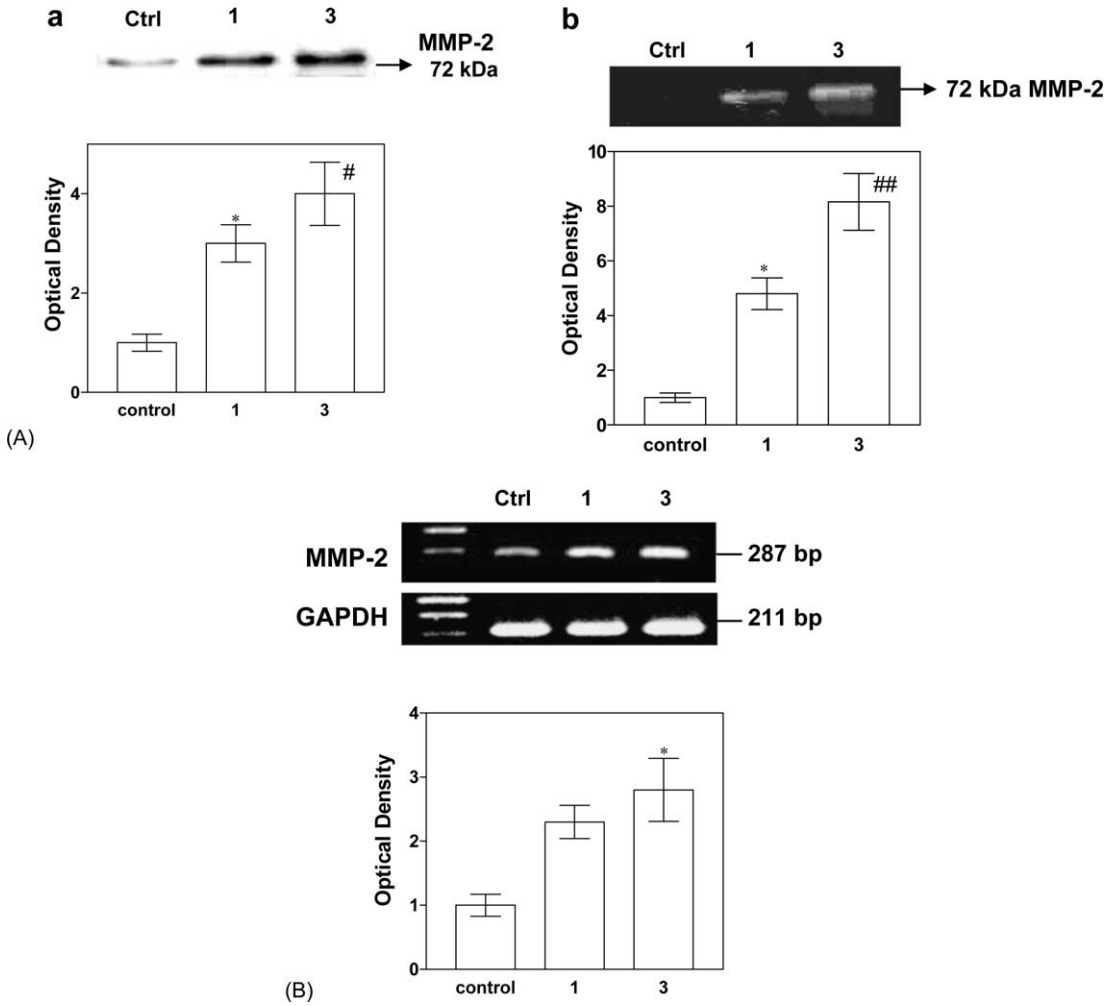

Fig. 5. OPN promotes MMP-2 expression and activity in stellate cells. (A) Cells were treated in the absence or presence of OPN (1, treated with 1 μg/ml OPN; 3, treated with 3 μg/ml OPN) and the conditioned media were collected. (a) MMP-2 protein determined using immunoblots; (b) MMP-2 activity determined by gelatin zymography. Results are means ± S.D. of three independent experiments. Statistical significance: $^{*}p < 0.05$, $^{\#}p < 0.01$, and $^{\#\#}p < 0.001$ vs. control conditions, as analyzed by one-way ANOVA and Tukey's multiple comparison tests. (B) Expression of MMP-2 mRNA in OPN-treated cells (1, treated with 1 μg/ml OPN; 3, treated with 3 μg/ml OPN) by RT-PCR analysis. A representative RT-PCR result is shown. Results are means ± S.D. from three independent experiments. The MMP-2 mRNA densitometry values were normalized to their respective GAPDH densitometry values. Statistical significance: $^{*}p < 0.05$ vs. control conditions, as analyzed by one-way ANOVA and Tukey's multiple comparison tests.

HSCs has provided profound insights into the cell activation mechanism. Until now, these HSC activation-related genes have been identified using differential display [27], subtractive hybridization [28,41,42] and proteome analysis [29]. In addition to these methods, we have previously undertaken a systematic survey of quiescent and activated HSCs to identify new genes associated with HSC activation [18,19,43] using an expression-profiling method [44] based on quantitative analysis of mRNA populations. Recently, a cDNA-microarray-based method was introduced for the high-throughput monitoring of gene expression [45]. This technology has revolutionized gene expression studies by providing the means with which to measure mRNA levels in thousands of genes simultaneously in simple and complex biological samples. In this study, using cDNA microarray analysis, we identified OPN as one of the genes that are upregulated in cultured activated HSCs.

Our study demonstrates that OPN is upregulated in the course of HSC activation at both the mRNA and protein levels. The overall involvement of OPN is also supported by its detection in, and its correlation with, the development of fibrosis in experimental models of liver fibrogenesis. Furthermore, we observed increased OPN protein in biliary atresia, with the most striking increases observed in Kupffer cell and HSCs in the necrotic areas.

The migration of ECM-producing cells represents a key event in wound healing and fibrogenic processes, and it is regulated by precise interactions with the ECM microenvironment [46,47]. Our study has demonstrated that OPN promotes migration and proliferation, two key mechanisms associated with liver fibrogenesis and HSC activation. It is noteworthy that endogenous OPN mRNA upregulation occurs during the spontaneous activation of HSC under standard culture conditions. OPN causes cell proliferation by interaction with its receptor αvβ3 integrin in various

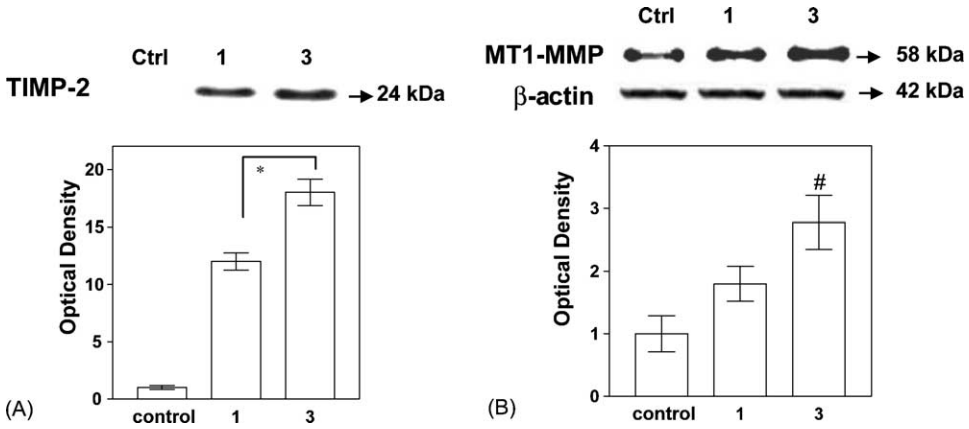

Fig. 6. OPN induces TIMP-2 and MT1-MMP expression in stellate cells. Cells were treated in the absence or presence of OPN (1, treated with 1 μg/ml OPN; 3, treated with 3 μg/ml OPN). (A) TIMP-2 expression was analyzed by immunoblotting of the conditioned media from cells. Results are means ± S.D. of three independent experiments. Statistical significance: $^{*}p < 0.001$ vs. control conditions, as analyzed by one-way ANOVA and Tukey's multiple comparison tests. (B) MT1-MMP expression was analyzed by immunoblotting of the lysates from cells. β-Actin was used as an internal control to normalize sample loading. Results are means ± S.D. of three independent experiments. Statistical significance: $^{\#}p < 0.05$ vs. control conditions, as analyzed by one-way ANOVA and Tukey's multiple comparison tests.

cell types [14]. Also, recent report indicated that αvβ3 integrin becomes expressed by HSCs during their activation in vitro [48]. Therefore, it is possible that ligand for αvβ3 integrin such as OPN is deposited in the space of Disse following liver injury and might ligate αvβ3 integrin on HSCs with the effect of supporting their proliferation, possibly in synergy with soluble growth factors such as PDGF released by Kupffer cells and platelets in response to injury. Further investigation will be required to clarify this point.

It is also noteworthy that very recently, a stimulatory role for OPN in MMP expression has been demonstrated in

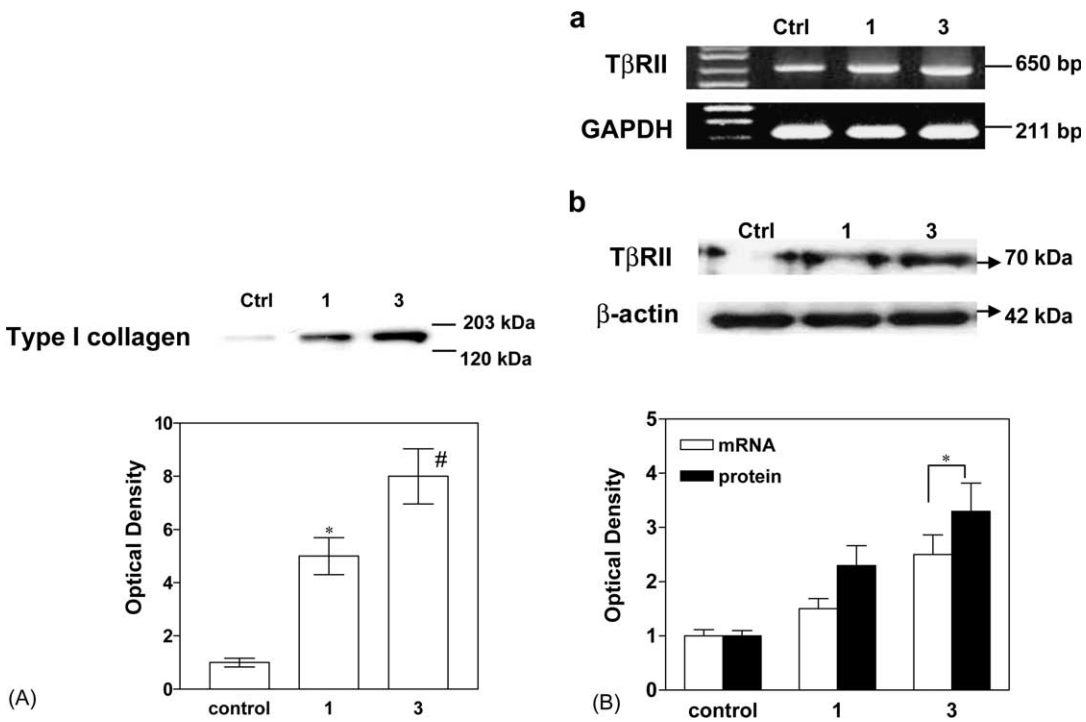

Fig. 7. (A) Effect of OPN on type I collagen protein production in HSCs. Cells were treated with OPN (1, treated with 1 μg/ml OPN; 3, treated with 3 μg/ml OPN) and type I collagen protein in the cell culture medium was measured by immunoblotting. Results are means ± S.D. of three independent experiments. Statistical significance: $^{*}p < 0.05$ and $^{\#}p < 0.01$ vs. control conditions, as analyzed by one-way ANOVA and Tukey's multiple comparison tests. (B) Effect of OPN on TβRII expression in HSCs. Cells were treated in the absence or presence of OPN (1, treated with 1 μg/ml OPN; 3, treated with 3 μg/ml OPN). (a) Expression of TβRII mRNA was determined by RT-PCR analysis. Integrity of the cDNA was confirmed by analysis of GAPDH mRNA. (b) TβRII protein expression was determined by immunoblotting. β-Actin was used as an internal control to normalize sample loading. Representative data of three independent experiments are shown. Results are means ± S.D. Statistical significance: $^{*}p < 0.05$ vs. control conditions, as analyzed by one-way ANOVA and Tukey's multiple comparison tests.

murine melanoma cells [49]. MMP are a family of Zn^{2+}-dependent endopeptidases that are responsible for remodeling the ECM, the degradation of ECM proteins, and the upregulation of MMP-2 activity, which accelerates HSC activation [5–7]. In this study, we demonstrated that recombinant OPN induces MMP-2 production and activation in a dose-dependent manner in HSCs. These data support our present finding that OPN induces HSC migration.

The activation of MMP-2 requires its localization to the cell surface and its cleavage by cell membrane-bound MT1-MMP. TIMP-2 is involved in this process by forming a receptor for MMP-2 [50]. We detected increased levels of TIMP-2 expression in OPN-treated HSCs. The balance between TIMP-2 and MMP-2 levels is critical in determining the activation status of MMP-2 because overexpression of TIMP-2 leads to MMP-2 inhibition. Using western blot analysis, we also detected increased levels of MT1-MMP expression. Increased MMP-2 activation reflects upregulation of MT1-MMP expression in OPN-treated cells, implying that OPN facilitates a shift in the balance toward increasing the proteolytic activity of MMP-2.

In this study, we also found that recombinant OPN induces type I collagen production in a dose-dependent manner in HSCs. TGF-β1 activates type I collagen promoters and increases the transcripts of ECM proteins such as collagen and fibronectin. TGF-β1 is synthesized and secreted in a latent, biologically inactive form, which must be activated before binding to TGF-β receptors. TGF-β signaling is initiated by the binding of this active cytokine to the TβRII, which phosphorylates and activates the type I TGF-β receptor [35,51]. The latter, in turn, phosphorylates Smad 2/3 proteins, which subsequently form a complex with Smad 4 and migrate to the nucleus to regulate the expression of target genes, including α1(I) collagen [52,53]. Therefore, we examined whether OPN has any role in the expression of TβRII in HSCs. In this study, we demonstrated that recombinant OPN did not increase TGF-β1 mRNA, but increased both TβRII mRNA and protein. Taken together, these data show that the effect of OPN on increasing type I collagen production in HSCs is mediated by the actions of OPN in increasing the effectiveness of TGF-β on fibrogenesis by means of an enhancement of TβRII.

In summary, we have demonstrated that OPN induces HSC migration and proliferation, which correlates with enhanced expression of MMP-2. We also provide evidence that OPN increases the gelatinolytic activity of MMP-2 by inducing TIMP-2 and MT1-MMP expression. Furthermore, we have demonstrated that OPN induces collagen synthesis in HSCs and that this effect is augmented by the OPN-mediated increase in TβRII expression. Collectively, the evidence points to a central role for OPN in liver fibrosis, and enhances the prospect of therapeutically affecting fibrogenetic processes by interrupting OPN expression or activity.

Acknowledgments

This work was supported by the Korea Food and Drug Administration Grant (KFDA-03142-BAS-906). The authors are grateful to Ms.H.M. Song who provided invaluable technical assistance for this study.

References

[1] Friedman SL. Molecular regulation of hepatic fibrosis; an integrated cellular response to tissue injury. J Biol Chem 2000;275:2247–50.
[2] Friedman SL. Hepatic stellate cells. Prog Liver Dis 1996;14:101–30.
[3] Olaso E, Friedman SL. Molecular regulation of hepatic fibrogenesis. J Hepatol 1998;29:836–47.
[4] Friedman SL, Roll FJ, Boyles J, Arenson DM, Bissell DM. Maintenance of differentiated phenotype of cultured rat hepatic lipocytes by basement membrane matrix. J Biol Chem 1989;264:10756–62.
[5] Arthur MJ, Stanley A, Iredale JP, Rafferty JA, Hembry RM, Friedman SL. Secretion of 72 kDa type IV collagenase/gelatinase by cultured human lipocytes. Analysis of gene expression, protein synthesis and proteinase activity. Biochem J 1992;287:701–7.
[6] Butler GS, Butler MJ, Atkinson SJ, Will H, Tamura T, van Westrum SS, et al. The TIMP2 membrane type 1 metalloproteinase receptor regulates the concentration and efficient activation of progelatinase A. J Biol Chem 1998;273:871–80.
[7] Werb Z. ECM and cell surface proteolysis: regulating cellular ecology. Cell 1997;91:439–42.
[8] Giachelli CM, Steitz S. Osteopontin: a versatile regulator of inflammation and biomineralization. Matrix Biol 2000;19:615–22.
[9] Denhardt DT, Guo X. Osteopontin: a protein with diverse functions. FASEB J 1993;7:1475–82.
[10] Prince CW. Secondary structure predictions for rat osteopontin. Connect Tissue Res 1989;21:15–20.
[11] Chen Y, Bal BS, Gorski JP. Calcium and collagen binding properties of osteopontin, bone sialoprotein, and bone acidic glycoprotein-75 from bone. J Biol Chem 1992;267:24871–8.
[12] Singh K, DeVouge MW, Mukherjee BB. Physiological properties and differential glycosylation of phosphorylated and nonphosphorylated forms of osteopontin secreted by normal rat kidney cells. J Biol Chem 1990;265:18696–701.
[13] Ritter NM, Farach-Carson MC, Butler WT. Evidence for the formation of a complex between osteopontin and osteocalcin. J Bone Miner Res 1992;7:877–85.
[14] Panda D, Kundu GC, Lee BI, Peri A, Fohl D, Chackalaparampil I, et al. Potential roles of osteopontin and αvβ3 integrin in the development of coronary artery restenosis after angioplasty. Proc Natl Acad Sci USA 1997;94:9308–13.
[15] Kawashima R, Mochida S, Matsui A, YouLuTuZ Y, Ishikawa K, Toshima K, et al. Expression of osteopontin in Kupffer cells and hepatic macrophages and Stellate cells in rat liver after carbon tetrachloride intoxication: a possible factor for macrophage migration into hepatic necrotic areas. Biochem Biophys Res Commun 1999;256:527–31.
[16] Gotoh M, Sakamoto M, Kanetaka K, Chuuma M, Hirohashi S. Overexpression of osteopontin in hepatocellular carcinoma. Pathol Int 2002;52:19–24.
[17] Ye QH, Qin LX, Forgues M, He P, Kim JW, Peng AC, et al. Predicting hepatitis B virus-positive metastatic hepatocellular carcinomas using gene expression profiling and supervised machine learning. Nat Med 2003;9:416–23.
[18] Lee SH, Seo GS, Park PH, Choi JY, Park YN, Kim HK, et al. Increased expression of *O*-acetyl disialoganglioside synthase during rat liver fibrogenesis relates to stellate cell activation. Biochem Biophys Res Commun 2003;303:954–61.

[19] Lee SH, Seo GS, Park YN, Sohn DH. Nephroblastoma overexpressed gene (NOV) expression in rat hepatic stellate cells. Biochem. Pharmacol., in press.
[20] Lee SH, Chae KS, Nan JX, Sohn DH. The increment of purine specific sodium nucleoside cotransporter mRNA in experimental fibrotic liver induced by bile duct ligation and scission. Arch Pharm Res 2000;23:613–9.
[21] Magaud JP, Sargent I, Mason DY. Detection of human white cell proliferative responses by immunoenzymatic measurement of bromodeoxyuridine uptake. J Immunol Methods 1988;106:95–100.
[22] Alessandri G, Raju KS, Gullino PM. Interaction of gangliosides with fibronectin in the mobilization of capillary endothelium. Possible influence on the growth of metastasis. Invasion Metastasis 1986;6:145–65.
[23] Fibbi G, Pucci M, Grappone C, Pellegrini G, Salzano R, Casini A, et al. Functions of the fibrinolytic system in human Ito cells and its control by basic fibroblast and platelet-derived growth factor. Hepatology 1999;29:868–78.
[24] Mazzocca A, Carloni V, Sciammetta S, Cordella C, Pantaleo P, Caldini A, et al. Expression of transmembrane 4 superfamily (TM4SF) proteins and their role in hepatic stellate cell motility and wound healing migration. J Hepatol 2002;37:322–30.
[25] Reif S, Lang A, Lindquist JN, Yata Y, Gabele E, Scanga A, et al. The role of focal adhesion kinase-phosphatidylinositol 3-kinase-akt signaling in hepatic stellate cell proliferation and type I collagen expression. J Biol Chem 2003;278:8083–90.
[26] Théret N, Lehti K, Musso O, Clément B. MMP2 activation by collagen I and concanavalin A in cultured human hepatic stellate cells. Hepatology 1999;30:462–8.
[27] Lang A, Schrum LW, Schoonhoven R, Tuvia S, Solis-Herruzo JA, Tsukamoto H, et al. Expression of small heat shock-protein αB-crystallin is induced after hepatic stellate cell activation. Am J Physiol Gastrointest Liver Physiol 2000;279:1333–42.
[28] Cassiman D, Roskams T, van Pelt J, Libbrecht L, Aertsen P, Crabbe T, et al. Alpha B-crystallin expression in human and rat hepatic stellate cells. J Hepatol 2001;35:200–7.
[29] Kristensen DB, Kawada N, Imamura K, Miyamoto Y, Tateno C, Seki S, et al. Proteome analysis of rat hepatic stellate cells. Hepatology 2000;32:268–77.
[30] Harada K, Ozaki S, Sudo Y, Tsuneyama K, Ohta H, Nakanuma Y. Osteopontin is involved in the formation of epithelioid granuloma and bile duct injury in primary biliary cirrhosis. Pathol Int 2003;53:8–17.
[31] Paradis V, Dargere D, Bonvoust F, Vidaud M, Segarini P, Bedossa P. Effect and regulation of connective tissue growth factor on hepatic stellate cells. Lab Invest 2002;82:767–73.
[32] Lauffenburger DA, Horwitz AF. Cell migration: a physically integrated molecular process. Cell 1996;84:359–69.
[33] Penttinen RP, Kobayashi S, Bornstein P. Transforming growth factor beta increases mRNA for matrix proteins both in the presence and in the absence of changes in mRNA stability. Proc Natl Acad Sci USA 1988;85:1105–8.
[34] Tang M, Potter JJ, Mezey E. Leptin enhances the effect of transforming growth factor beta in increasing type I collagen formation. Biochem Biophys Res Commun 2002;297:906–11.
[35] Massague J, Chen YG. Controlling TGF-β signaling. Genes Dev 2000;14:627–44.
[36] Eng FJ, Friedman SL, Fibrogenesis I. New insights into hepatic stellate cell activation: the simple becomes complex. Am J Physiol Gastrointest Liver Physiol 2000;279:7–11.
[37] Pinzani M, Gentilini P. Biology of hepatic stellate cells and their possible relevance in the pathogenesis of portal hypertension in cirrhosis. Semin Liver Dis 1999;19:397–410.
[38] Kawada N. The hepatic perisinusoidal stellate cell. Histol Histopathol 1997;12:1069–80.
[39] Gressner AM. The cell biology of liver fibrogenesis—an imbalance of proliferation, growth arrest and apoptosis of myofibroblasts. Cell Tissue Res 1998;292:447–52.
[40] Svegliati-Baroni G, Ridolfi F, Di Sario A, Casini A, Marucci L, Gaggiotti G, et al. Insulin and insulin-like growth factor-1 stimulate proliferation and type I collagen accumulation by human hepatic stellate cells: differential effects on signal transduction pathways. Hepatology 1999;29:1743–51.
[41] Ratziu V, Lalazar A, Wong L, Dang Q, Collins C, Shaulian E, et al. Zf9, a Kruppel-like transcription factor upregulated in vivo during early hepatic fibrosis. Proc Natl Acad Sci USA 1998;95:9500–5.
[42] Ikeda K, Kawada N, Wang YQ, Kadoya H, Nakatani K, Sato M, et al. Expression of cellular prion protein in activated hepatic stellate cells. Am J Pathol 1998;153:1695–700.
[43] Lee SH, Chae KS, Sohn DH. Identification of expressed sequence tags of genes expressed highly in the activated hepatic stellate cell. Arch Pharm Res 2004;27:422–8.
[44] Okubo K, Hori N, Matoba R, Niiyama T, Fukushima A, Kojima Y, et al. Large scale cDNA sequencing for analysis of quantitative and qualitative aspects of gene expression. Nat Genet 1992;2:173–9.
[45] Schena M, Shalon D, Davis RW, Brown PO. Quantitative monitoring of gene expression patterns with a complementary DNA microarray. Science 1995;270:467–70.
[46] Carloni V, Romanelli RG, Pinzani M, Laffi G, Gentilini P. Focal adhesion kinase and phospholipase C gamma involvement in adhesion and migration of human hepatic stellate cells. Gastroenterology 1997;112:522–31.
[47] Marra F, Gentilini A, Pinzani M, Choudhury GG, Parola M, Herbst H, et al. Phosphatidylinositol 3-kinase is required for platelet-derived growth factor's actions on hepatic stellate cells. Gastroenterology 1997;112:1297–306.
[48] Zhou X, Murphy FR, Gehdu N, Zhang J, Iredale JP, Benyon RC. Engagement of αvβ3 integrin regulates proliferation and apoptosis of hepatic stellate cells. J Biol Chem 2004;279:23996–4006.
[49] Philip S, Bulbule A, Kundu GC. Osteopontin stimulates tumor growth and activation of promatrix metalloproteinase-2 through nuclear factor-kappa B-mediated induction of membrane type 1 matrix metalloproteinase in murine melanoma cells. J Biol Chem 2001;276:44926–35.
[50] Hernandez-Barrantes S, Toth M, Bernardo MM, Yurkova M, Gervasi DC, Raz Y, et al. Binding of active (57 kDa) membrane type 1-matrix metalloproteinase (MT1-MMP) to tissue inhibitor of metalloproteinase (TIMP)-2 regulates MT1-MMP processing and pro-MMP-2 activation. J Biol Chem 2000;275:12080–9.
[51] Baker JC, Harland RM. From receptor to nucleus: the Smad pathway. Curr Opin Genet Dev 1997;7:467–73.
[52] Ignotz RA, Massague J. Transforming growth factor-beta stimulates the expression of fibronectin and collagen and their incorporation into the extracellular matrix. J Biol Chem 1986;261:4337–45.
[53] Czaja MJ, Weiner FR, Flanders KC, Giambrone MA, Wind R, Biempica L, et al. In vitro and in vivo association of transforming growth factor-β1 with hepatic fibrosis. J Cell Biol 1989;108:2477–82.